Motion Control of a Pair of Cylindrical Manipulators in a Constrained 3-dimensional Workspace

Avinesh Prasad
School of Computing, Information and Mathematical Sciences
The University of the South Pacific
Fiji
Email: avinesh.prasad@usp.ac.fj

Bibhya Sharma
School of Computing, Information and Mathematical Sciences
The University of the South Pacific
Fiji
Email: bibhya.sharma@usp.ac.fj

Jito Vanualailai
School of Computing, Information and Mathematical Sciences
The University of the South Pacific
Fiji
Email: vanualailai@usp.ac.fj

Abstract—**In this paper we utilize the Lyapunov-based Control Scheme (LbCS) to solve the motion control problem of a pair of cylindrical manipulators working in a constrained 3-dimensional workspace. The end-effectors of each manipulator is required to move from initial to final positions whilst obeying all singularities and constraints associated with the system. We also consider fixed and moving obstacles in the workspace which the robots have to avoid at all times. The stability of the system is studied using the Direct Method of Lyapunov, where as computer simulations are used to verify the effectiveness of the proposed nonlinear control laws.**

Keywords: Cylindrical manipulators, Lyapunov-based Control Scheme, Minimum Distance Technique, Stability.

I. Introduction

A robot manipulator is an electronically controlled mechanism made up of multiple rigid links connected by different joints [1]. The two basic types of joints commonly found in literature are (i) revolute (R) that allows relative rotation between two links and (ii) prismatic (P) that provides a linear sliding (translational) movement between two links [2]. The joint combinations give rise to various 3-dimensional manipulator configuration which are categorized as cartesian (PPP), cylindrical (RPP), spherical (RRP), SCARA (RRP) and articulated (RRR) manipulators. The reader can refer to [3] for a detailed explanation of these categories of manipulators.

The robot manipulators nowadays play a vital role in the manufacturing industries. Jobs that require high precision and repeatability such as packaging, labelling and assembling of products are carried out by robots. In the recent years, there has been a high demand for industrial robots to perform repetitious (such as pick and place of objects), dirty (such as repairing sewage pipes), hazardous (such as welding and spray painting) and difficult tasks (such as assembly or replacement of electronic parts). The robot manipulators have the ability to perform a given task with high accuracy, autonomy, reliability, independently and responsibly.

Autonomous motion control of manipulator arms is not an easy task due to the system and workspace constraints, non-reachability of end-effectors and the associated mechanical singularities. Moreover, if workspace contains fixed and moving obstacles, then the motion control becomes more difficult since each body of the robot needs to avoid an obstacle. Researchers have used various methods to construct the kinematics model of manipulator arms. The kinematic model appearing in literature are mainly constructed through (but not limited to): (i) forward kinematics where the coordinates of the end-effector is determined using the joint angles; and (ii) inverse kinematics where the joint angles is determined using the coordinates of the end-effector; and (iii) velocity kinematics which involve translational and angular velocities of the joints.

We present a few relevant and prominent works from literature. Dahari et.al in [4] modelled the forward and inverse kinematics of a KUKA KR-16KS robotic arm in the application of a simple welding process. Liqing et.al in [5] solved the inverse kinematics for 6-DOF manipulator by the method of sequential retrieval. Altintas et.al [6] designed and implemented the 3-axis cylindrical and cartesian coordinate robot manipulators actuated with stepper motors and developed Matlab program for controlling the designed robot manipulators. Gonz et.al [7] designed a sliding mode controller that was robust against perturbations and parameter variations, had finite time convergence, and was easy to implement. Other noteworthy works involving the motion control of manipulator arms include that of Gupta [8], Seraji and Bon [9], Ohashi et al. [10] and Petar et al. [13].

In this paper, we plan and control the motion of a pair of cylindrical manipulators working in a constrained workspace whilst obeying system constraints and singularities, and simultaneously avoiding fixed and moving obstacles. The motion of the manipulators are modelled as a system of first-order nonlinear differential equations. We then utilize the Lyapunov-based Control Scheme to extract a set of nonlinear, time-invariant, continuous control laws to generate collision-free motions of the cylindrical manipulators. The reasons for utilizing this scheme is mainly due to its simplicity and elegance. Moreover, the analytic representation of system singularities and constraints are easy, and the extraction of control laws is straightforward.

The reminder of the paper is organized as follows: The kinematic model describing the motion of the two manipulator arms is derived in Section II. In Section III, the attractive potential functions are given which inherently allows the end-effectors to converge to their designated targets. The various types of obstacles and the associated potential functions are discussed in Section IV. Section V provides a Lyapunov function or total potentials of the system and the nonlinear control laws are designed such that the system is stable. Simulations results are provided in Section VI followed by conclusion and remarks on future work in Section VII.

II. The Manipulator Model

The 3-dimensional cylindrical manipulator arm, shown in the Fig. 1, is adopted from [11]. The first joint is revolute which produces a rotation about the base, while the second and third joints are prismatic. We assume that each manipulator arm consists of 4 links made up of uniform slender rods [11]; revolute first link of fixed length, a prismatic second and fourth link with varying lengths, and a third link to provide support to the fourth link. With reference to Fig. 1, we assume that (for $i = 1, 2$):

(i) The position of the center of the fixed base is $(a_i, b_i, 0)$;
(ii) The angular position of the links 3 and 4 is $\theta_i(t)$, measured counterclockwise from the w_1-axis;
(iii) Links 1 and 3 have fixed lengths of ℓ_1 and ℓ_2, respectively.
(iv) Links 2 and 4 have varying lengths of $r_{i1}(t)$ and $r_{i2}(t)$, respectively.
(v) The coordinate of the end-effector is (x_i, y_i, z_i).

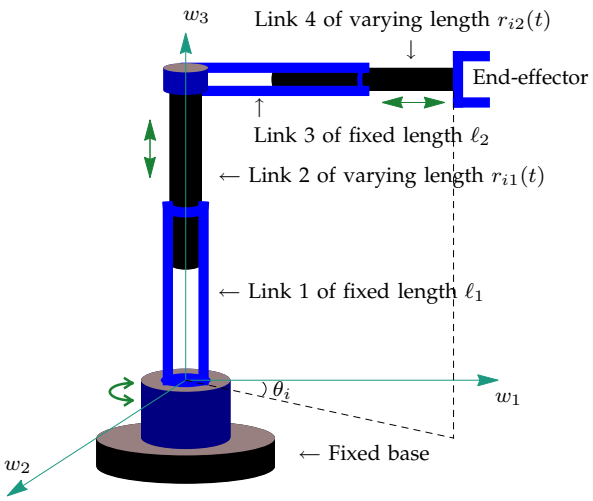

Fig. 1. Schematic representation of a 3-Dimensional Cylindrical Manipulator mounted on a fixed base.

The position of the end-effectors can be expressed as

$$\begin{aligned} x_i(t) &= a_i + (\ell_2 + r_{i2}(t)) \cos\theta_i(t), \\ y_i(t) &= b_i + (\ell_2 + r_{i2}(t)) \sin\theta_i(t), \\ z_i(t) &= \ell_1 + r_{i1}(t). \end{aligned}$$

Suppose the ith end-effector is moving at a velocity of $v_i = u_{i1}\mathbf{i} + u_{i2}\mathbf{j} + u_{i3}\mathbf{k}$, where u_{i1}, u_{i2} and u_{i3} are the w_1, w_2 and w_3 components, respectively, of v_i. The kinematic model for the 3-dimensional cylindrical manipulator arm derived by Prasad et.al in [11] is

$$\left.\begin{aligned} \dot{r}_{i1} &= u_{i3}, \\ \dot{r}_{i2} &= u_{i1}\cos\theta_i + u_{i2}\sin\theta_i, \\ \dot{\theta}_i &= \frac{u_{i2}\cos\theta_i - u_{i1}\sin\theta_i}{r_{i2} + \ell_2}, \\ r_{i1}(0) &= z_i(0) - \ell_1, \\ r_{i2}(0) &= \sqrt{(x_i(0) - a_i)^2 + (y_i(0) - b_i)^2} - \ell_2, \\ \theta_i(0) &= \text{atan2}\,(y_i(0) - b_i, x_i(0) - a_i) \end{aligned}\right\} \quad (1)$$

for $i = 1, 2$. System (1) is a description of the instantaneous velocities of the manipulator. Here u_{i1}, u_{i2} and u_{i3}, $i = 1, 2$ are classified as the nonlinear velocity controllers. We shall use the vector notation $\mathbf{x}(t) = (r_{11}(t), r_{12}(t), \theta_1(t), r_{21}(t), r_{22}(t), \theta_2(t)) \in \mathbb{R}^6$ to refer to the positional configurations of the the two manipulator arms.

Our main objective is to use the Lyapunov-based control scheme, which was proposed by Sharma in [12], to derive the controllers for the manipulator arms. The main idea behind the control scheme is to design an appropriate Lyapunov function which acts as an energy function. We construct attractive and avoidance functions for the attraction to target(s) and repulsion from various obstacles, respectively. The Lyapunov function

is the sum of all attractive and repulsive potential functions. We note that the repulsive potential functions are designed as ratios with the obstacle avoidance function in the denominator of each ratio and a positive *tuning parameter* in the numerator. We then design the control laws such that the Lyapunov function is decreasing for all $t \geq 0$ and vanishes to zero as $t \to \infty$. The design of the nonlinear control laws is captured in Figure 2.

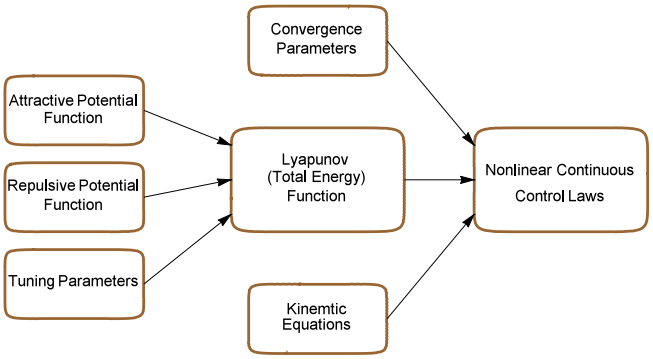

Fig. 2. Block diagram explaining the control scheme.

III. Target Attractions

We affix targets for the end-effectors to reach after some time $t > 0$. The targets are spheres of center (p_{i1}, p_{i2}, p_{i3}) and radius r_T which is described as

$$\begin{aligned} T_i &= \{(w_1, w_2, w_3) \in \mathbb{R}^3 : \\ &\quad (w_1 - p_{i1})^2 + (w_2 - p_{i2})^2 + (w_3 - p_{i3})^2 \leq r_T^2\}. \end{aligned}$$

For attractions to the target, we consider

$$V_i(\mathbf{x}) = \frac{1}{2}\left[(x_i - p_{i1})^2 + (y_i - p_{i2})^2 + (z_i - p_{i3})^2\right]. \quad (2)$$

We shall see later that when the total potentials is designed, $V_i(\mathbf{x})$ will act as an attractive potential function, attracting the end-effectors to their designated target.

IV. Avoidance of Obstacles

In this section, we look at some possible forms of obstacles that can be encountered by the manipulators on their way to the respective targets. In particular, we will consider artificial obstacles (mechanical singularities), fixed and moving obstacles and the workspace restrictions.

A. Artificial Obstacles

The mechanical singularities associated with the system give rise to artificial obstacles. We note that links 2 and 4 can not be detached from links 1 and 3, respectively. Similarly, the end-effectors can not go inside the link 3. Thus, we impose the following conditions:

1) $0 < r_{i1} < R_{1\max}$,
2) $0 < r_{i2} < R_{2\max}$,

where $R_{1\max}$ and $R_{2\max}$ are, respectively, the maximal extensions of links 1 and 3. These conditions give rise to the following artificial obstacles:

$$\begin{aligned} AO_1 &= \{r_{i1} \in \mathbb{R} : r_{i1} \leq 0 \text{ or } r_{i1} \geq R_{1\max}\}, \\ AO_2 &= \{r_{i2} \in \mathbb{R} : r_{i2} \leq 0 \text{ or } r_{i2} \geq R_{2\max}\}. \end{aligned}$$

To avoid these artificial obstacles, the following potential functions is constructed.

$$S_{i1}(\mathbf{x}) = r_{i1}, \qquad S_{i2}(\mathbf{x}) = r_{i2}, \quad (3a\text{-}b)$$
$$S_{i3}(\mathbf{x}) = R_1 - r_{i1}, \qquad S_{i4}(\mathbf{x}) = R_2 - r_{i2} \quad (3c\text{-}d)$$

for $i = 1, 2$. We will see later in Section V that each of these functions will be added as a ratio to a Lyapunov function of the system. Note that along any trajectories generated by system (1), a Lyapunov function, say $L(\mathbf{x}(t))$, is always non-negative and decreasing for all $t \geq 0$. Hence $L(\mathbf{x}(t)) \leq L(\mathbf{x}(0)) < \infty$. Now consider the effect of the ratio α_{11}/S_{11} for some positive constant α_{11}. When $r_{11}(t) \to 0$, this ratio will increase making $L(\mathbf{x}(t)) \to \infty$. This leads to a contradiction since $L(\mathbf{x}(t)) < \infty$. Thus we conclude that $S_{11}(\mathbf{x}) > 0$ and hence $r_{11}(t) > 0$.

Henceforth, for each obstacle, we will construct an appropriate potential function that will appear in the denominator of a ratio in the Lyapunov function of system (1).

B. Moving Obstacles

When multiple robots operate in a shared workspace, then each robot becomes a dynamic obstacle to others [13]. To avoid collisions between the two moving manipulators, it is important that the end-effectors must avoid all four links of the adjacent manipulator. We utilize the minimum distance technique (MDT) proposed by Sharma in [12]. The basic idea is to find a point on each of the four links of the jth manipulator that is closest to the ith end-effector. At any time $t \geq 0$, the closest point on each link (and hence the entire jth manipulator) will be avoided by the ith end-effector.

To find a point on each link of jth manipulator that is closest to the end-effector of the ith manipulator, we need to minimize the functions

$$\begin{aligned} D_{ij} &= \|(x_i, y_i, z_i) - (a_j, b_j, \lambda_{ij} z_j)\|, \\ D^*_{ij} &= \|(x_i, y_i, z_i) - (X^*_{ij}, Y^*_{ij}, z_j)\| \end{aligned}$$

where

$$\begin{aligned} X^*_{ij} &= a_j + \lambda^*_{ij}(\ell_2 + r_{j2})\cos\theta_j, \\ Y^*_{ij} &= b_j + \lambda^*_{ij}(\ell_2 + r_{j2})\sin\theta_j, \\ z_j &= \ell_1 + r_{j1}. \end{aligned}$$

The functions D_{ij} and D^*_{ij} are minimum if

$$\begin{aligned} \lambda_{ij} &= \min\left\{\max\left\{0, \frac{z_i}{z_j}\right\}, 1\right\} \quad \text{and} \\ \lambda^*_{ij} &= \min\left\{\max\left\{0, \frac{(x_i - a_j)\cos\theta_j}{\ell_2 + r_{j2}} + \frac{(y_i - b_j)\sin\theta_j}{\ell_2 + r_{j2}}\right\}, 1\right\}. \end{aligned}$$

For the ith end-effector to avoid collisions with the four links of jth manipulator, we construct the potential functions

$$Q_{ij}(\mathbf{x}) = \frac{1}{2}\left[(x_i - a_j)^2 + (y_i - b_j)^2 + (z_i - \lambda_{ij} z_j)^2\right] \quad (4a)$$

$$R_{ij}(\mathbf{x}) = \frac{1}{2}\left[(x_i - X^*_{ij})^2 + (y_i - Y^*_{ij})^2 + (z_i - z_j)^2\right] \quad (4b)$$

for $i, j \in \{1, 2\},\ i \neq j$.

C. Fixed Obstacles

Let us fix $q \in \mathbb{N}$ spherical obstacles within the boundaries of the workspace.

Definition 1: The lth obstacle (for $l = 1, 2, \ldots, q$) is a sphere with center (o_{l1}, o_{l2}, o_{l3}) and radius ro_l, and is defined as the set

$$\begin{aligned} FO_l &= \{(w_1, w_2, w_3) \in \mathbb{R}^3 : \\ &\quad (w_1 - o_{l1})^2 + (w_2 - o_{l2})^2 + (w_3 - o_{l3})^2 \leq ro_l^2\}. \end{aligned}$$

For the manipulators to avoid an obstacle, it suffices to find a point on links 3 and 4 of that is closest to the obstacle. For this, we again utilize MDT to minimize the distance function

$$d_{il} = \|(x^*_{il}, y^*_{il}, z_i) - (o_{l1}, o_{l2}, o_{l3})\|$$

where

$$\begin{aligned} x^*_{il} &= a_i + \gamma_{il}(\ell_2 + r_{i2})\cos\theta_i, \\ y^*_{il} &= b_i + \gamma_{il}(\ell_2 + r_{i2})\sin\theta_i. \end{aligned}$$

The function d_{il} is minimum provided

$$\gamma_{il} = \min\left\{\max\left\{0, \frac{(o_{l1} - a_i)\cos\theta_i + (o_{l2} - b_i)\sin\theta_i}{\ell_2 + r_{i2}}\right\}, 1\right\}.$$

For the manipulators to avoid collisions with any obstacle, we construct the potential function

$$W_{il}(\mathbf{x}) = \frac{1}{2}\left[\left\|(x^*_{il}, y^*_{il}, z_i) - (o_{l1}, o_{l2}, o_{l3})\right\|^2 - ro_l^2\right] \quad (5)$$

for $i = 1, 2$ and $l = 1, 2, \ldots, q$.

D. Workspace restrictions

Our workspace is a fixed, closed and bounded cubical region, defined, for some constants η_1, η_2, and η_3 as

$$\begin{aligned} WS &= \{(w_1, w_2, w_3) \in \mathbb{R}^3 : \\ &\quad -\eta_1 \leq w_1 \leq \eta_1, -\eta_2 \leq w_2 \leq \eta_2, 0 \leq w_3 \leq \eta_3\}. \end{aligned}$$

We assume that the two manipulators are fixed within the boundaries of the workspace. The end-effector of each manipulator is required to stay within the workspace at all time $t \geq 0$. As such, the following potential functions is constructed.

$$B_{i1}(\mathbf{x}) = x_i + \eta_1, \qquad B_{i2}(\mathbf{x}) = \eta_1 - x_i, \quad (6a\text{-}b)$$

$$B_{i3}(\mathbf{x}) = y_i + \eta_2, \qquad B_{i4}(\mathbf{x}) = \eta_2 - y_i, \quad (6c\text{-}d)$$

$$B_{i5}(\mathbf{x}) = z_i, \qquad B_{i6}(\mathbf{x}) = \eta_3 - z_i, \quad (6e\text{-}f)$$

for $i = 1, 2$.

V. Design of the Non-linear Control Laws

We now define a Lyapunov function by combining all the potential functions (2) - (6) and introducing *tuning parameters*, $\alpha_{ik} > 0$, $\beta_{il} > 0$, $\zeta_{ij} > 0$, $\xi_{ij} > 0$ and $\mu_{is} > 0$, where $i, j, k, l, r \in \mathbb{N}$. A Lyapunov function or total potentials for system (1) is

$$\begin{aligned} L(\mathbf{x}) = \sum_{i=1}^{2}\Bigg\{V_i(\mathbf{x})\Bigg[1 + \sum_{k=1}^{4}\frac{\alpha_{ik}}{S_{ik}(\mathbf{x})} + \sum_{l=1}^{q}\frac{\beta_{il}}{W_{il}(\mathbf{x})} \\ + \sum_{\substack{j=1 \\ j\neq i}}^{2}\left(\frac{\zeta_{ij}}{Q_{ij}(\mathbf{x})} + \frac{\xi_{ij}}{R_{ij}(\mathbf{x})}\right) + \sum_{r=1}^{6}\frac{\mu_{ir}}{B_{ir}(\mathbf{x})}\Bigg]\Bigg\} \end{aligned} \quad (7)$$

The Lyapunov function is positive, continuous and bounded over the domain

$$\begin{aligned} D &= \big\{\mathbf{x} \in \mathbb{R}^6 :\ S_{ik}(\mathbf{x}) > 0,\ U_{il}(\mathbf{x}) > 0, \\ &\quad Q_{ij}(\mathbf{x}) > 0,\ R_{ij}(\mathbf{x}) > 0,\ B_{ir}(\mathbf{x}) > 0\big\}. \end{aligned}$$

Now let $\mathbf{e}_i = (r^*_{i1}, r^*_{i2}, \theta^*_i)$, where

$$\begin{aligned} r^*_{i1} &= p_{i3} - \ell_1, \\ r^*_{i2} &= \sqrt{(p_{i1} - a_i)^2 + (p_{i2} - b_i)^2} - \ell_2, \\ \theta^*_i &= \text{atan2}\,(p_{i2} - b_i, p_{i1} - a_i) + 2\pi n \text{ for some } n \in \mathbb{Z} \end{aligned}$$

be the configuration of the ith arm when its end-effector reaches the target. Then $\mathbf{e} = (r^*_{11}, r^*_{12}, \theta^*_1, r^*_{21}, r^*_{22}, \theta^*_2)$ is an equilibrium point of system (1). We now design the control laws such that $\mathbf{e}$ is a stable equilibrium point. That is, any solution of system (1) starting close to $\mathbf{e}$ remains near the equilibrium point at all times. This is illustrated in Theorem 1.

Theorem 1: The equilibrium point $\mathbf{e}$ of system (1) is stable provided the controllers u_{i1}, u_{i2} and u_{i3}, $(i = 1, 2)$ are defined as

$$\left.\begin{aligned} u_{i1} &= -\frac{1}{\delta_{i1}}\left(\frac{\partial L}{\partial r_{i2}}\cos\theta_i - \frac{\partial L}{\partial \theta_i}\frac{\sin\theta_i}{\ell_2 + r_{i2}}\right), \\ u_{i2} &= -\frac{1}{\delta_{i2}}\left(\frac{\partial L}{\partial r_{i2}}\sin\theta_i + \frac{\partial L}{\partial \theta_i}\frac{\cos\theta_i}{\ell_2 + r_{i2}}\right), \\ u_{i3} &= -\frac{1}{\delta_{i3}}\frac{\partial L}{\partial r_{i1}}, \end{aligned}\right\} \tag{8}$$

where $\delta_{i1} > 0$, $\delta_{i2} > 0$, $\delta_{i3} > 0$ are called the convergence parameters.

Proof: We note that the Lyapunov function $L(\mathbf{x})$ defined in (7) is continuous, positive and bounded over the domain D. Also $L(\mathbf{x})$ has continuous first partial derivatives in the region D in the neighborhood of the equilibrium point $\mathbf{e}$ of system (1). Moreover, in the region D, we see that $L(\mathbf{e}) = 0$ and $L(\mathbf{x}) > 0$ for all $\mathbf{x} \neq \mathbf{e}$. Next, the time-derivative of $L(\mathbf{x})$ is

$$\begin{aligned} \dot{L}(\mathbf{x}) &= \sum_{i=1}^{2}\left\{\frac{\partial L}{\partial z_i}\frac{\partial z_i}{\partial r_{i1}}\dot{r}_{i1} + \left(\frac{\partial L}{\partial x_i}\frac{\partial x_i}{\partial r_{i2}} + \frac{\partial L}{\partial y_i}\frac{\partial y_i}{\partial r_{i2}}\right)\dot{r}_{i2}\right. \\ &\quad \left. + \left(\frac{\partial L}{\partial x_i}\frac{\partial x_i}{\partial \theta_i} + \frac{\partial L}{\partial y_i}\frac{\partial y_i}{\partial \theta_i}\right)\dot{\theta}_i\right\} \\ &= \sum_{i=1}^{2}\left\{\left(\frac{\partial L}{\partial r_{i2}}\cos\theta_i - \frac{\partial L}{\partial \theta_i}\frac{\sin\theta_i}{\ell_2 + r_{i2}}\right)u_{i1}\right. \\ &\quad \left. + \left(\frac{\partial L}{\partial r_{i2}}\sin\theta_i + \frac{\partial L}{\partial \theta_i}\frac{\cos\theta_i}{\ell_2 + r_{i2}}\right)u_{i2} + \frac{\partial L}{\partial r_{i1}}u_{i3}\right\} \\ &= -\sum_{i=1}^{2}\left\{\delta_{i1}u_{i1}^2 + \delta_{i2}u_{i2}^2 + \delta_{i3}u_{i3}^2\right\}. \end{aligned}$$

It is clear that in the region D, $\dot{L}(\mathbf{x}) \leq 0$ and $\dot{L}(\mathbf{e}) = 0$. Hence $\mathbf{e}$ is a stable equilibrium point of system (1).

VI. Simulation

The set of differential equations given in system (1) is numerically integrated using the fourth-order Runge-Kutta method and the feasible trajectories are generated as shown in Fig. 3. The simulations shown in Fig. 3 illustrate the movement of two manipulator arms to their respective targets while avoiding the obstacles in a bounded workspace. The smooth trajectories are obtained through appropriate manipulation of the control and convergence parameters. The details of different parameters used in the simulations are given in Table I.

Fig. 3(a) shows the initial state of the two robot. In Fig. 3(b), we have simulated the trajectories of the two robots showing the movement of the end-effectors from their initial positions to the designated targets. The two robots had to avoid each other on their path to the targets. In Fig. 3(c), we placed a spherical obstacle to obstruct the movement of the two manipulator arms. Due to the unique and tailored nature of the control laws in (8), the two robots avoided the spherical obstacle, avoided collision between each other and converged to the equilibrium point.

TABLE I
Values of the different parameters used in the simulation.

Initial and Final Positions	
Initial Positions	$\mathbf{x}(0) = (0.5, 0.5, -\pi/2, 0.5, 0.5, \pi/4)$.
Target Positions	$(p_{11}, p_{12}, p_{13}) = (-143.8)$ and $(p_{21}, p_{22}, p_{23}) = (1 - 43.8)$.
Fixed Obstacle Parameters	
Center	$(0_{11}, 0_{12}, 0_{13}) = (0, 0, 3)$.
Radius	$ro_1 = 0.5$.
Robot Parameters	
Dimensions	$\ell_1 = 2$ m, $\ell_2 = 4$ m, $(a_1, b_1) = (4, 0)$, $(a_2, b_2) = (-4, 0)$.
Other Parameters	
Workspace dimensions	$-50 \leq z_1 \leq 50$, $0 \leq z_2 \leq 50$.
Convergence parameters	$\delta_{ij} = 10$, $i = 1, 2, 3$ and $j = 1, 2$.
Maximal extensions	$R_{1\max} = 2$ m and $R_{2\max} = 4$ m.

Fig. 4 show explicitly the time evolution of the controllers along the trajectory of the mobile manipulators. We notice the asymptotic convergence of the controllers at the final state implying the effectiveness of the new controllers. Fig. 5 shows the Lyapunov function and its time derivative along the system trajectory. The graph of $L(\mathbf{x})$ is continuous and bounded. Moreover, we see that $L(\mathbf{e}) = 0$ and $L(\mathbf{x}) > 0$ for all $\mathbf{x} \neq \mathbf{e}$. From the time-derivative graph, we notice that $\dot{L}(\mathbf{x}) \leq 0$ and $\dot{L}(\mathbf{e}) = 0$.

VII. Conclusion

This paper presented a new solution to the motion control problem of a pair of cylindrical manipulators working in a constrained 3-dimensional workspace. The robots also avoided fixed and moving obstacles while moving from initial to final states. To ensure that each component of a robot does not collide with obstacles, the minimum distance technique was utilized. The set of nonlinear control laws were derived using the Lyapunov-based Control Scheme. The proposed method is verified using computer simulations.

Future work in this area includes deriving control laws for synchronous movement of the autonomous system in cooperation, pick and place of objects and considering partially known or fully unknown workspace.

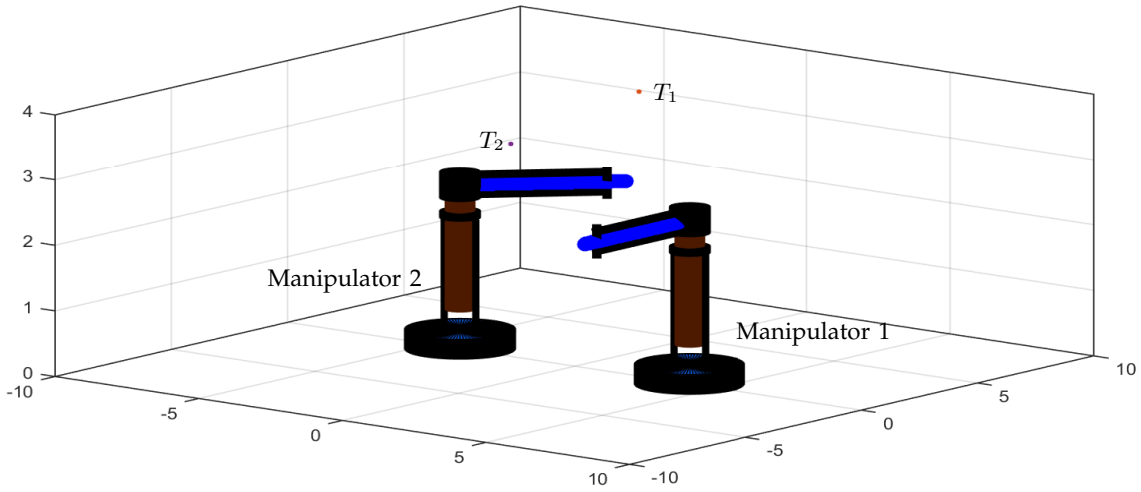

(a) Initial Configuration.

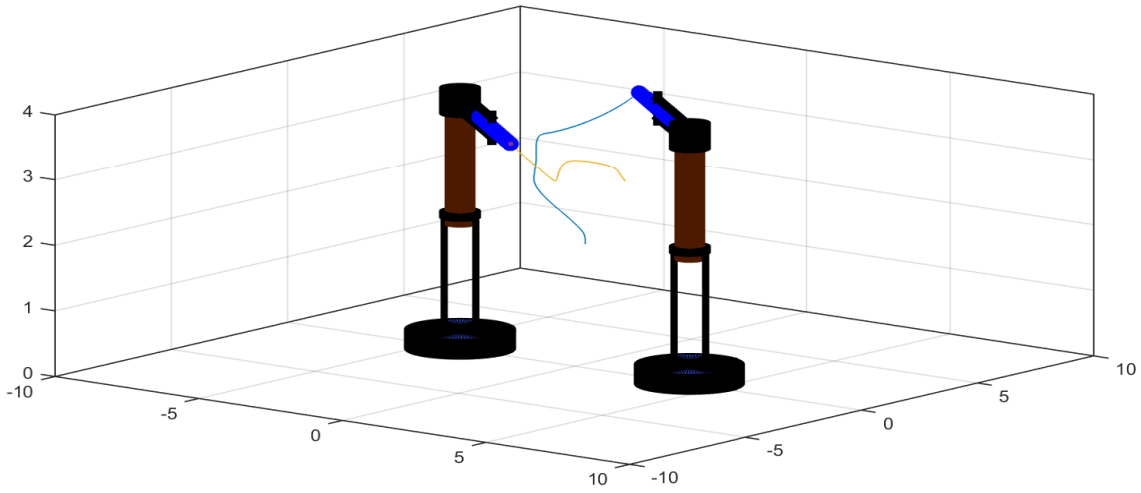

(b) Convergence of the manipulators to the targets in the absence of fixed obstacles.

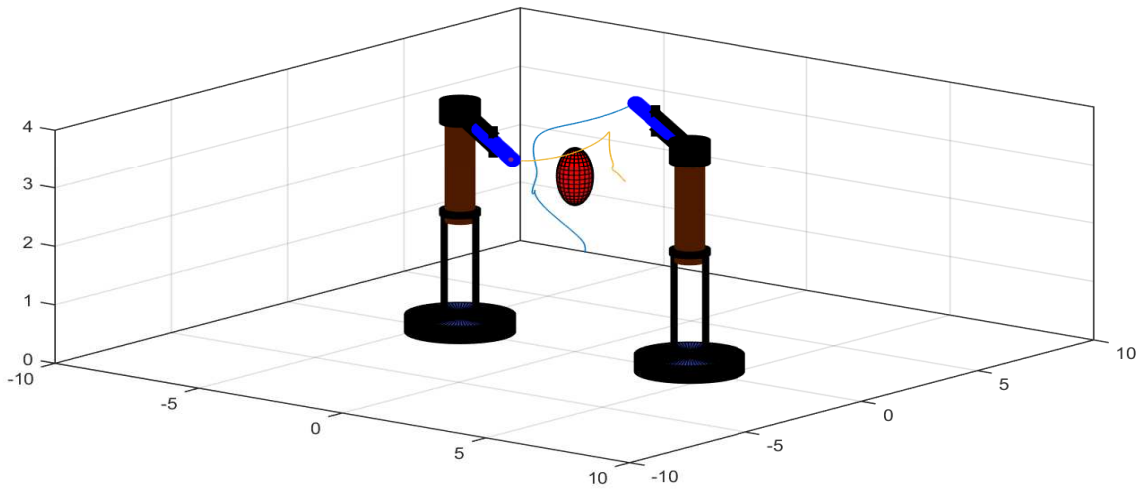

(c) Convergence of the manipulators to the targets in the presence of a fixed obstacles.

Fig. 3. Movement of the manipulator arms from initial to final configurations.

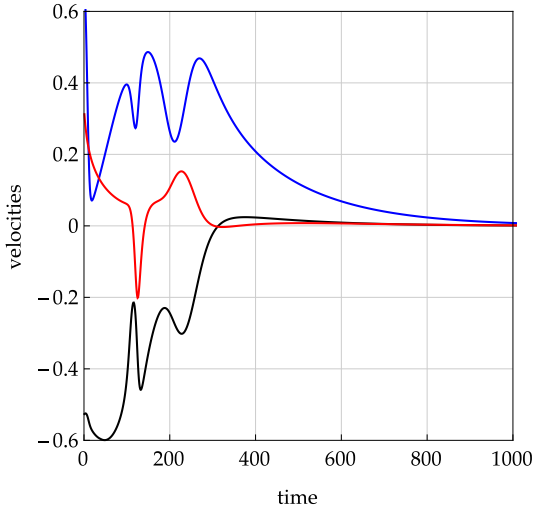

(a) Controllers u_{11} in black, u_{12} in blue and u_{13} in red.

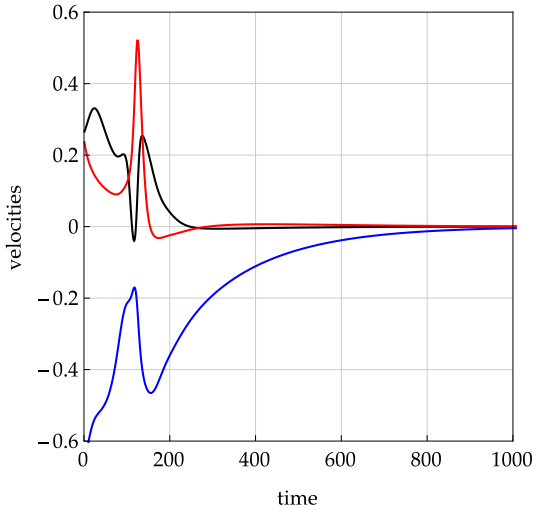

(b) Controllers u_{21} in black, u_{22} in blue and u_{23} in red.

Fig. 4. Evolution of the nonlinear controllers along the trajectories shown in Figure 3(c).

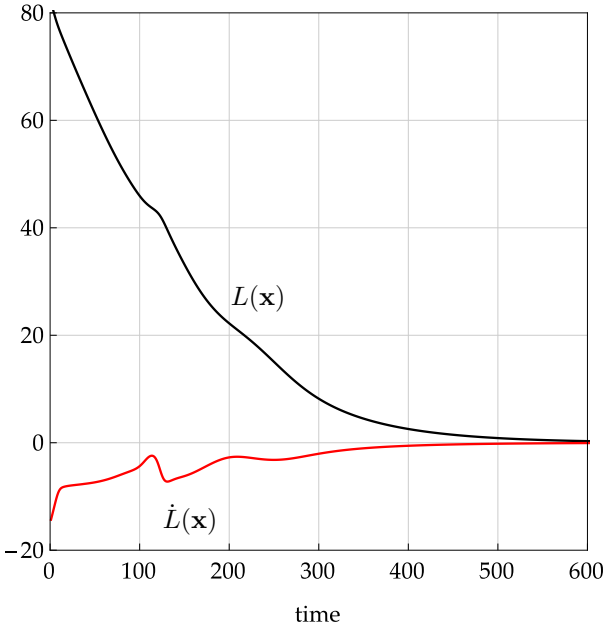

Fig. 5. Evolution of the Lyapunov function and its time derivative along the trajectories shown in Figure 3(c).

References

[1] S. Tejomurtula and S. Kak. Inverse kinematics in robotics using neural networks. *Information Science*, 116(2-4):147–164, January 1999.

[2] J. Vanualailai, S. Nakagiri, and J. Ha. A solution to two-dimension findpath problem. *Dynamics and Stability of Systems*, 13:373–401, 1998.

[3] Mark W. Spong. *Robot Dynamics and Control*. John Wiley & Sons, Inc., New York, NY, USA, 1st edition, 1989.

[4] M. Dahari and J. D. Ta. Forward and inverse kinematics model for robotic welding process using kr-16ks kuka robot. In *2011 Fourth International Conference on Modeling, Simulation and Applied Optimization*, pages 1–6, April 2011.

[5] N. Liqing and H. Qingjiu. Inverse kinematics for 6-dof manipulator by the method of sequential retrieval. In *2012 International Conference on Mechanical Engineering and Material Science*, pages 255–258, November 2012.

[6] A. Altintas. A new approach to 3-axis cylindrical and cartesian type robot manipulators in mechatronics education. In *Electronics & Electrical Engineering*, 2010.

[7] L. González-Jiménez, O. Carbajal-Espinosa, A. Loukianov, and E. Bayro-Corrochano. Robust pose control of robot manipulators using conformal geometric algebra. *Advances in Applied Clifford Algebras*, 24(2):533–552, 2014.

[8] K.K. Gupta. Fast collision avoidance for manipulator arms: a sequential search strategy. *Robotics and Automation, IEEE Transactions on*, 6(5):522 –532, oct 1990.

[9] H. Seraji and B. Bon. Real-time collision avoidance for position-controlled manipulators. *Robotics and Automation, IEEE Transactions on*, 15(4):670 –677, aug 1999.

[10] E. Ohashi, T. Aiko, T. Tsuji, H. Nishi, and K. Ohnishi. Collision avoidance method of humanoid robot with arm force. *Industrial Electronics, IEEE Transactions on*, 54(3):1632 –1641, june 2007.

[11] A. Prasad, B. Sharma, and J. Vanualailai. Motion planning and control of a point-mass robot in a 3-dimensional space with application to a cylindrical manipulator. In *2015 2nd Asia-Pacific World Congress on Computer Science and Engineering (APWC on CSE)*, pages 1–7, Dec 2015.

[12] B. Sharma. *New Directions in the Applications of the Lyapunov-based Control Scheme to the Findpath Problem*. PhD thesis, University of the South Pacific, Suva, Fiji Islands, July 2008.

[13] P. Curkovic, B. Jerbic, and T. Stipancic. Co-evolutionary algorithm for motion planning of two industrial robots with overlapping workspaces. *International Journal of Advanced Robotic Systems*, 10(1):55, 2013.